

## Mechanistic aspects of ligand substitution on $[(\text{H}_2\text{O})(\text{tap})_2\text{RuORu}(\text{tap})_2(\text{H}_2\text{O})]^{2+}$ {tap=2-(m-tolylazo)pyridine} ion by three glycine-containing dipeptides in aqueous medium at physiological pH

ARUP MANDAL, SUBALA MONDAL, PARNAJYOTI KARMAKAR, BIPLAB K BERA, SUBHASIS MALLICK and ALAK K GHOSH\*

Department of Chemistry, The University of Burdwan, Burdwan 713 104, India  
e-mail: alakghosh2002@yahoo.co.in

MS received 24 July 2011; revised 21 October 2011; accepted 31 October 2011

**Abstract.** The interaction of the title complex with selected glycine-containing dipeptides(L-L/H) such as glycyL-glycine(L-L<sup>1</sup>H), glycyL-L-alanine (L-L<sup>2</sup>H) and glycyL-L-leucine(L-L<sup>3</sup>H) has been studied spectrophotometrically in aqueous medium as a function of [substrate complex], [ligand] and temperature. The reaction has been monitored at 600 nm where the spectral difference between the reactant and product is a maximum. At pH 7.4, the interaction with studied dipeptides shows two parallel steps. i.e., it shows a non-linear dependence on the concentration of dipeptides; both processes are ligand-dependent. The rate constants for the processes are:  $k_1 \sim 10^{-3} \text{ s}^{-1}$  and  $k_2 \sim 10^{-5} \text{ s}^{-1}$ . The activation parameters were calculated from Eyring plots. Based on the kinetic and activation parameters an associative interchange mechanism is proposed for the interaction processes. From the temperature dependence of the outer sphere association equilibrium constant, the thermodynamic parameters were also calculated. The product of the reaction has been characterized by IR and ESI-mass spectroscopic analysis.

**Keywords.** Ligand substitution; dipeptides; *cis*-diaqua-*bis*-{2-(m-tolylazo)pyridine} ruthenium(II); kinetics.

### 1. Introduction

Most new drugs are carbon-based compounds but there is an increasing realization that many metal ions are involved in natural biological processes and that there is much scope for the design of metal-based therapeutic agents.<sup>1,2</sup> In general, the nature of the metal ion, its oxidation state, and the types and number of bound ligands, can all exert a critical influence on the biological activity of a metal complex.<sup>3,4</sup> An understanding of how these factors affect biological activity should enable the design of metal complexes with specific medicinal properties. The wide spectrum of contrasting biological activity amongst platinum complexes<sup>1,5,6</sup> and the clinical success of platinum (II) diam (m) ine complexes, e.g., *cis*-platin, as anticancer drugs provide a good illustration of this point. Although platinum complexes are now widely used for the treatment of cancer, the development of drug resistance, the toxic side-effects of *cis*-platin, and the lack of activity of platinum compounds against several types of cancer are problems which need to be overcome. This provides the impetus for

the search for anticancer activity amongst complexes of other metals. Ruthenium, rhodium, iridium and palladium complexes have also been reported to have considerable biological activity.<sup>7,8</sup> Of them, ruthenium complexes seem to be less toxic than *cis*-platin.<sup>9,10</sup> Different studies reveal that a number of ruthenium compounds serve as bacterial mutagens, capable of damaging genetic material and also have some biological demands.<sup>11–29</sup> Ruthenium(III) is a pro-drug which is reduced to ruthenium(II) under the hypoxic environment of the affected cells where the chemical environment is also aggressive. On the other hand, the halo-complexes are hydrolysed to aqua variety in the cell. The hydrolysis side products are toxic. The aqua complexes of ruthenium(II) may be better choice. The reaction is straight forward and the side effects are reduced. But the practical problem is that, although ruthenium is less toxic than other Pt-metal complexes, most of them are oxidized to ruthenium(III) at a pH 7.4 (physiological pH). In this context, our title complex is unique. So far as biological activity is concerned, DNA is not the only target. Studies with RNA, amino acids, dipeptides and other active components in the body are also equally important.

\*For correspondence

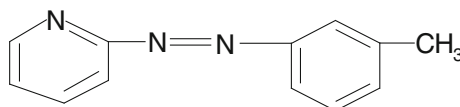
Some of the main chemical features of Ru compounds that might be relevant for their biological activity are listed below. Two main oxidation states are accessible for ruthenium species in physiological solution: Ru(II) ( $d^6$ , diamagnetic) and Ru(III) ( $d^5$ , paramagnetic). In both oxidation states the Ru ion is six-coordinate with octahedral geometry (while Pt(II) is square planar) and, like Pt(II), has good affinity for nitrogen and sulphur ligands. Ru(II) species will remain unoxidized in air only if good  $\pi$ -acceptor ligands are present. Broadly speaking, Ru complexes have kinetics for ligand exchange similar to those of Pt(II) species. It is also generally accepted that Ru(II) complexes are less inert compared to the corresponding Ru(III) species. Finally, the ability of ruthenium to mimic iron in binding to many biological molecules, including serum proteins (e.g., transferrin and albumin) is believed to contribute to the general low toxicity of ruthenium drugs.<sup>30</sup> In the assumption that this active Ru(II) compounds have to coordinate to some biological target in order to exert their anticancer activity, they are to be considered, like Pt drugs, as prodrugs.

We report here the interaction of some dipeptides having a different set of donor atoms. The work has been done in aqueous medium and at physiological

pH (7.4) under which conditions most of the ruthenium(II) complexes are oxidized to ruthenium(III); but the +2 state of the metal ion in (1) is quite stable due to the presence of an excellent  $\pi$ -acceptor<sup>31</sup> ligand, tap{tap=2-(m-tolylazo)pyridine}.

## 2. Materials and methods

The compound *cis*-diaqua-*bis*-{2-(m-tolylazo)pyridine} ruthenium(II) diperchlorate, monohydrate, *cis*-[Ru(tap)<sub>2</sub>(H<sub>2</sub>O)<sub>2</sub>](ClO<sub>4</sub>)<sub>2</sub>·H<sub>2</sub>O was prepared following the literature method<sup>32,33</sup> and the reacting complex ion [(H<sub>2</sub>O)(tap)<sub>2</sub>RuORu(tap)<sub>2</sub>(H<sub>2</sub>O)]<sup>2+</sup> (1) was prepared *in situ* at pH 7.4.



tap {tap=2-(m-tolylazo) pyridine}.

The product [(tap)<sub>2</sub>Ru(μ-O)(μ-L<sup>1</sup>H)Ru(tap)<sub>2</sub>]<sup>+</sup> (2) of the reaction between complex (1) and glycyl-glycine was prepared by mixing the reactants in 1:1, 1:2, 1:3, 1:5 and 1:10 ratios and thermostated at 50°C for 72 h. The spectrum of (2) (figure 1) shows good complexation between glycyl-glycine and (1).

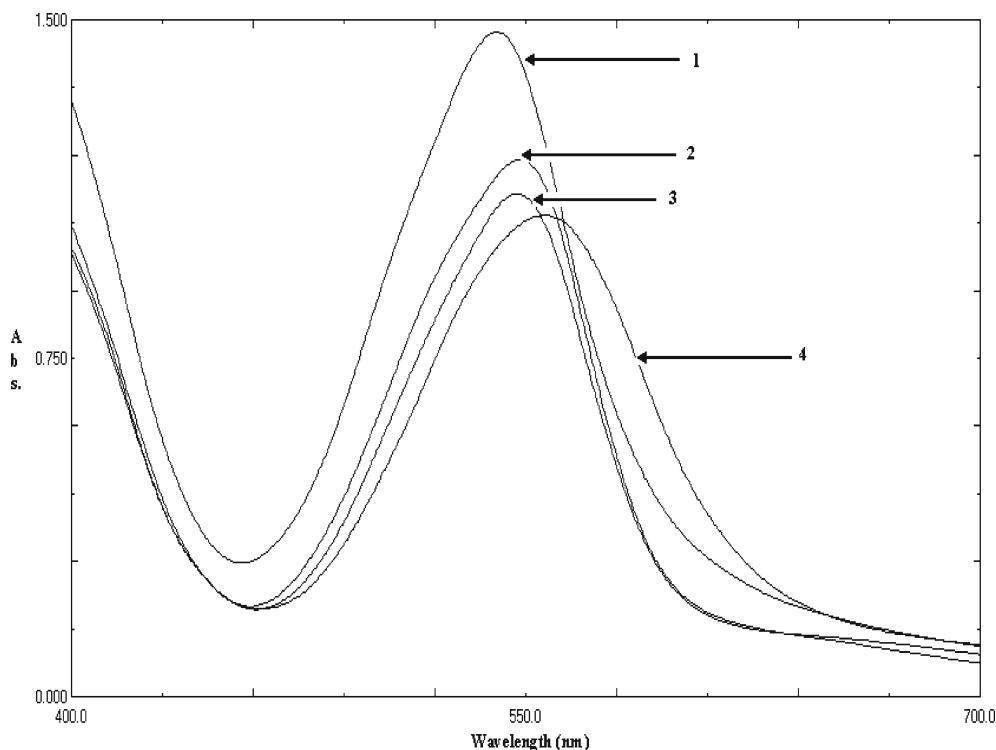


**Figure 1.** Spectral differences between substrate complex and products at 60°C after 2 h. (1). [(H<sub>2</sub>O)(tap)<sub>2</sub>RuORu(tap)<sub>2</sub>(H<sub>2</sub>O)]<sup>2+</sup> = 1.0 × 10<sup>-4</sup> M, [glycyl-glycine] = 3.0 × 10<sup>-3</sup> M; (2). [(H<sub>2</sub>O)(tap)<sub>2</sub>RuORu(tap)<sub>2</sub>(H<sub>2</sub>O)]<sup>2+</sup> = 1.0 × 10<sup>-4</sup> M, [glycyl-alanine] = 3.0 × 10<sup>-3</sup> M; (3). [(H<sub>2</sub>O)(tap)<sub>2</sub>RuORu(tap)<sub>2</sub>(H<sub>2</sub>O)]<sup>2+</sup> = 1.0 × 10<sup>-4</sup> M, [glycyl-leucine] = 3.0 × 10<sup>-3</sup> M; (4). [(H<sub>2</sub>O)(tap)<sub>2</sub>RuORu(tap)<sub>2</sub>(H<sub>2</sub>O)]<sup>2+</sup> = 1.0 × 10<sup>-4</sup> M; pH = 7.4

### 3. Kinetics

Kinetic measurements were carried out on a Shimadzu UV 1601 spectrophotometer attached to a thermoelectric cell temperature controller (model TCA 240A, accuracy  $\pm 0.1^\circ$ ) the conventional mixing technique was followed and pseudo-first order conditions were employed throughout. The progress of the reaction was followed by measuring the decrease in absorbance at 600 nm, where the spectral difference between the substrate and the product complex is maximum. The  $k_{1(obs)}$  and  $k_{2(obs)}$  values were calculated graphically (figures 2 and 3) using the method of Weyh and Hamm.<sup>34</sup> We took the help of Origin 6.0 for other calculations. The rate data represented as an average of duplicate runs are reproducible within  $\pm 4\%$ .

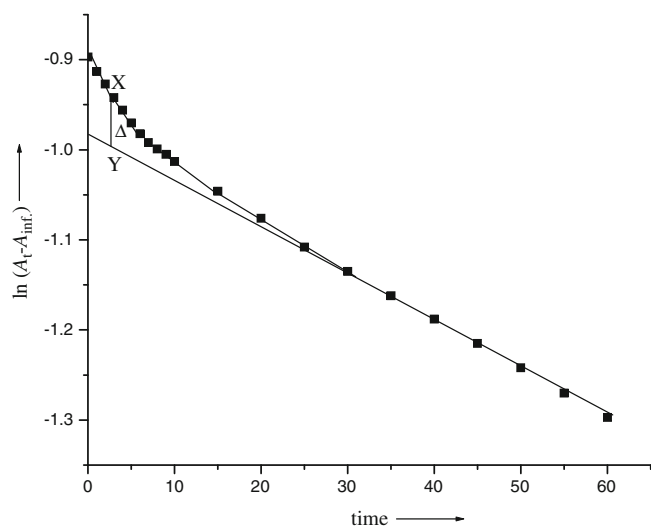


**Figure 2.** A typical plot of  $\ln(A_t - A_\infty)$  versus time  $t$ . [complex] =  $1.0 \times 10^{-4}$  mol dm $^{-3}$ , [glycyl-glycine] =  $2.0 \times 10^{-3}$  mol dm $^{-3}$ ; pH = 7.4, Temp. = 35°C.

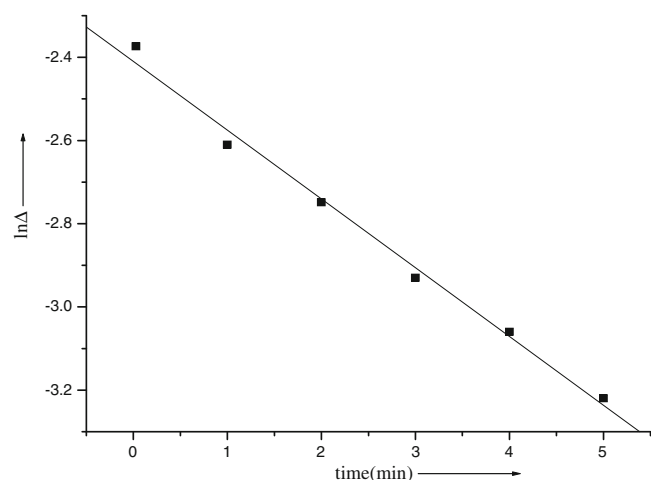
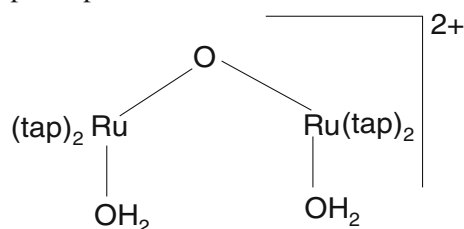


**Figure 3.** A typical plot of  $\ln\Delta$  versus time  $t$ . [complex] =  $1.0 \times 10^{-4}$  mol dm $^{-3}$ , [glycyl-glycine] =  $2.0 \times 10^{-3}$  mol dm $^{-3}$ ; pH = 7.4, Temp. = 50°C.

### 4. Results and discussion

The  $pK_a$  values of the ligands L-L<sup>1</sup>H, L-L<sup>2</sup>H and L-L<sup>3</sup>H are 3.21, 8.13<sup>35,36</sup> 3.07, 8.12<sup>37</sup> and 3.18, 8.14<sup>38</sup>, respectively at 25°C. From the  $pK_a$  values of all the ligands we can say that at pH 7.4, all these three ligands remain in the zwitter ion form.

On the other hand, first acid dissociation equilibrium of the complex  $[Ru(tap)_2(H_2O)_2]^{2+}$  is 6.6<sup>39</sup> at 25°C. At pH 7.4, the complex ion exists in dimeric oxo-bridged form,  $[(H_2O)(tap)_2RuORu(tap)_2(H_2O)]^{2+}$ .<sup>40-44</sup> The oxo-bridge formation is solely dependent on pH. Electrochemical studies show that there is pH potential domain, where the  $\mu$ -oxo structures stay intact. Variable temperature study does not show any effect, which is in line with the fact that oxo-bridge formation is solely pH-dependent.<sup>45,46</sup>



At constant temperature, pH (7.4) and fixed concentration of complex (I) the  $\ln(A_t - A_\infty)$  versus time ( $t$ ) plot for different ligand concentration indicates a two-step process. Both are dependent on the incoming ligand concentration, and with increasing ligand concentration a limiting rate is reached. Job's method of complexation indicates a 2:1 metal-ligand ratio in the product complex. This is possible only when the reaction occur through two parallel paths. The rate constant for such process can be evaluated by assuming the following scheme 1.

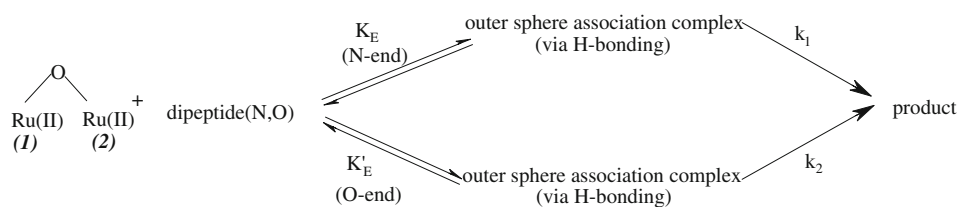
In the starting complex there are two equivalent ruthenium (II) centres. Now the ligand has two donor centres (N and O). As ruthenium(II) is a soft centre, during the ligation two donor centres attack in two parallel speeds ( $k_1$  and  $k_2$ ) which is shown in the mechanism and conclusion section.

#### 4.1 Calculation of $k_1$ value

The rate constant for this path was calculated from the absorbance data using the Weyh and Hamm<sup>34</sup> equation.

$$(A_t - A_\infty) = a_1 \exp(-k_{1(obs)}t) + a_2 \exp(-k_{2(obs)}t), \quad (1)$$

where  $a_1$  and  $a_2$  are constants that depend upon the rate constants and extinction coefficients.



**Scheme 1.** Possible reaction pathways for the interaction of dipeptides with the title complex.

Values of  $a_2 \exp(-k_{2(\text{obs})}t)$  at different times (when  $t$  is small) were obtained from the linear portion of the curve (figure 2) extended to  $t$  equals zero, i.e.,

$$a_2 \exp(-k_{2(\text{obs})}t) = (A_t - A_\infty)_{\text{limiting}}.$$

Therefore values of  $(A_t - A_\infty) - a_2 \exp(-k_{2(\text{obs})}t)$  were calculated from X and Y values (figure 2) at different  $t$ ;

$$\Delta = a_1 \exp(-k_{1(\text{obs})}t) \quad (2)$$

or,  $\ln \Delta = \text{constant} - k_{1(\text{obs})}t$

$k_{1(\text{obs})}$  was then derived from the slope of  $\ln \Delta$  versus time, for small values of  $t$  (figure 3).

A similar procedure was applied for each glycylglycine concentration in the  $1.0 \times 10^{-3} \text{ mol dm}^{-3}$  to  $5.0 \times 10^{-3} \text{ mol dm}^{-3}$  range using the experimental conditions specified in table 1. The  $k_{1(\text{obs})}$  values for all given ligands are presented in table 1.

The rate increases with increase in  $[\text{L-L}^1\text{H}]$  and reaches a limiting value (figure 4). The limiting rate is probably due to the completion of outer sphere association complex formation. Since the metal ion reacts with its immediate environment, further change in  $[\text{L-L}^1\text{H}]$  beyond the saturation point will not affect the reaction

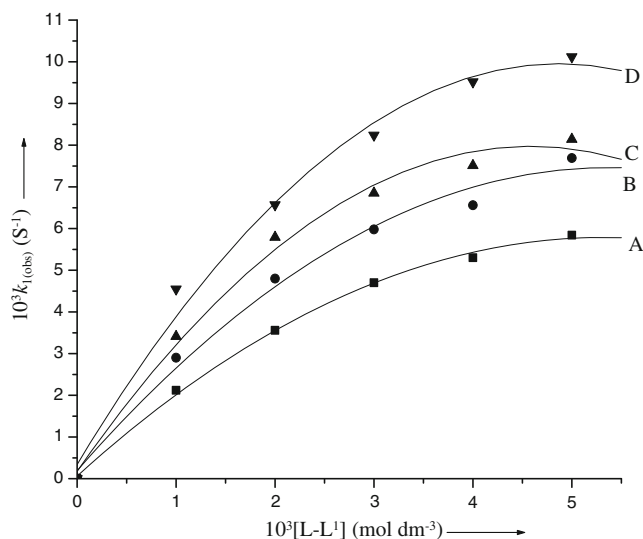
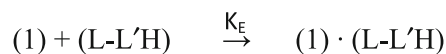
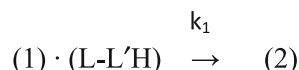


**Figure 4.** Plot of  $k_{1(\text{obs})}$  versus glycyl-glycine  $[\text{L-L}^1\text{H}]$  at different temperature, A = 35, B = 40, C = 45 and D = 50°C.

rate. The outer sphere association complex may be stabilized through H-bonding. Based on the experimental findings, the following scheme 2 may be proposed for the path (1)  $\rightarrow$  (2) ( $k_1$  path);



Outer sphere association complex



**Scheme 2.** Possible reaction sequence for the interaction of dipeptides with the title complex.

Based on the above scheme a rate expression can be derived.

$$d[2]/dt = k_1 K_E [(\text{H}_2\text{O})(\text{tap})_2\text{RuORu}(\text{tap})_2(\text{H}_2\text{O})^{2+}] \times [\text{L-L}^1\text{H}] \quad (3)$$

and

$$d[2]/dt = k_{1(\text{obs})} [(\text{H}_2\text{O})(\text{tap})_2\text{RuORu}(\text{tap})_2(\text{H}_2\text{O})^{2+}]_T \quad (4)$$

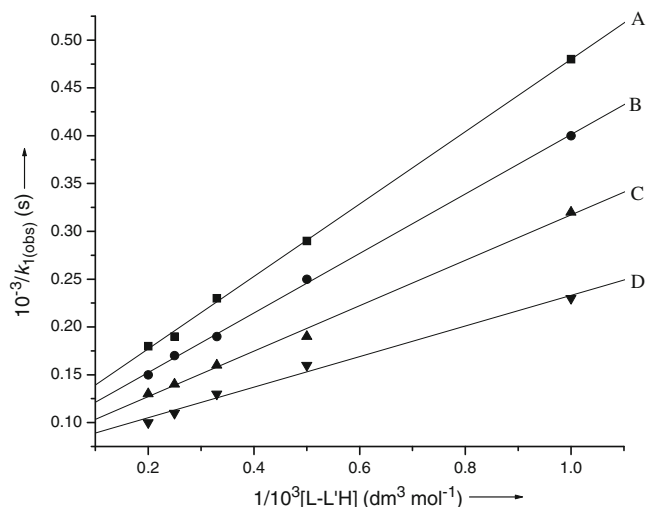


**Figure 5.** Plot of  $1/k_{1(\text{obs})}$  against  $1/[\text{L-L}^1\text{H}]$ , A = 35, B = 40, C = 45 and D = 50°C.

**Table 1.**  $10^3 k_{1(\text{obs})}$  values for different ligand concentrations at different temperatures. [Complex 1] =  $1.00 \times 10^{-4}$  mol dm $^{-3}$ , pH = 7.4, ionic strength = 0.1 mol dm $^{-3}$  NaClO $_4$ .

Ligand	Temperature	$10^3$ [ligand] (mol dm $^{-3}$ )				
		1.00	2.00	3.00	4.00	5.00
L-L $^1$ H	35	2.12	3.56	4.70	5.30	5.84
	40	2.90	4.80	5.98	6.56	7.69
	45	3.41	5.79	6.85	7.51	8.14
	50	4.55	6.57	8.24	9.52	10.12
L-L $^2$ H	35	2.10	3.52	4.52	5.28	5.55
	40	2.80	4.54	5.90	6.25	7.00
	45	3.35	5.59	6.54	7.31	8.13
	50	4.52	6.52	8.22	9.39	10.00
L-L $^3$ H	35	2.08	3.45	4.35	5.26	5.56
	40	2.50	4.00	5.26	5.88	6.67
	45	3.10	5.39	6.25	7.14	7.69
	50	4.35	6.25	8.00	9.29	9.59

Where  $T$  stands for total concentration of Ru(II). We can then write,

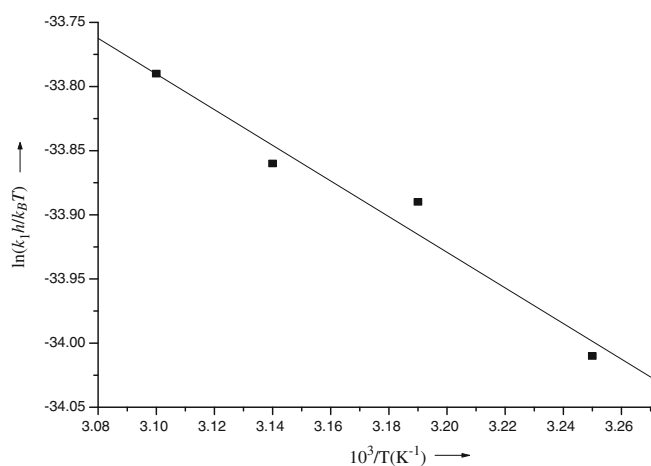
$$k_{1(\text{obs})} = k_1 K_E [L - L'H] / (1 + K_E [L - L'H]), \quad (5)$$

where  $k_1$  is the rate constant for the  $k_1$  path, i.e., the rate constant for the interchange of outer sphere complex to the inner sphere complex;  $K_E$  is the outer sphere association equilibrium constant.

The equation can be represented as

$$1/k_{1(\text{obs})} = 1/k_1 + 1/k_1 K_E [L - L'H]. \quad (6)$$

The plot of  $1/k_{1(\text{obs})}$  against  $1/[L-L'H]$  should be linear with an intercept of  $1/k_1$  and slope  $1/k_1 K_E$ . This was found to be the case at all temperatures studied. The  $k_1$  and  $K_E$  values were calculated from the intercept and slope (figure 5) and are collected in table 3.

**Figure 6.** Eyring plot for  $k_1$  (For L-L $^1$ H).

## 4.2 Calculation of $k_2$ value

The similar procedure (calculation of  $k_1$ ) was applied to calculate the  $k_2$  values. The rate constants for this path were calculated from the latter linear portions of the graphs and are collected in table 2. This is again dependent on  $[L-L'H]$  and shows a limiting value at higher ligand concentrations. The intermediate here is also possibly stable through H-bonding between coordinated water and the approaching amino acids dipolar ion.

In a parallel reaction two paths overlap each other. But during the calculation of the first path the contribution from the second path is negligible. On the other hand, when we are calculating the rate constant for the second path the first path is already complete. Thus there is no problem in calculating  $k_1$  and  $k_2$ .

The  $k_2$  and  $K'_E$  for the second path is calculated in a manner similar to Equation (6) and data are presented in table 3.

Based on the experimental findings, a two-step interchange associative mechanism is proposed for the substitution process. In the first path, an outer sphere association complex is formed between the ligand and the two ruthenium (II) centres, which is stabilized by the H-bonding between the incoming dipeptides and the coordinated aqua molecules. Now the interchange of the ligand from the outer sphere to the inner sphere occurs.

## 4.3 Effect of temperature

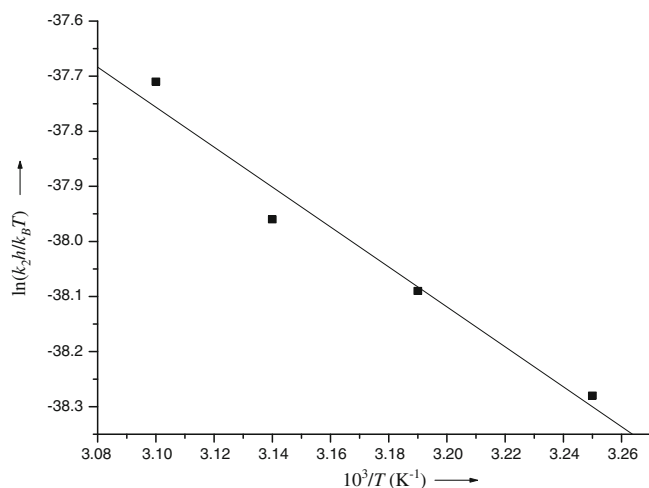
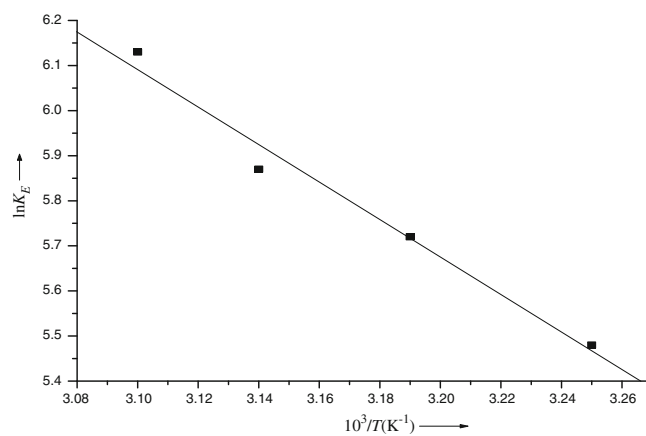
The reaction was studied at four different temperatures for different ligand concentrations and the results are listed in tables 1 and 2. The two rate constants  $k_1$  and

**Table 2.**  $10^5 k_{2(\text{obs})}$  values for different ligand concentrations at different temperatures. [Complex 1] =  $1.00 \times 10^{-4}$  mol dm $^{-3}$ , pH = 7.4, ionic strength = 0.1 mol dm $^{-3}$  NaClO $_4$ .

Ligand	Temperature	$10^3$ [ligand] (mol dm $^{-3}$ )				
		1.00	2.00	3.00	4.00	5.00
L-L $^1$ H	35	3.13	5.15	6.70	7.90	8.50
	40	4.80	7.20	9.36	11.37	11.98
	45	5.56	8.77	11.23	12.50	13.62
	50	7.46	12.19	15.39	16.50	17.48
L-L $^2$ H	35	3.00	4.83	6.37	7.52	8.10
	40	4.09	6.19	8.34	10.35	10.93
	45	4.87	7.76	10.45	11.87	12.23
	50	6.80	11.09	14.37	15.40	16.28
L-L $^3$ H	35	2.89	4.72	6.25	7.40	7.99
	40	3.80	6.06	8.22	10.22	10.49
	45	4.76	7.65	10.34	11.75	12.00
	50	6.56	11.00	14.28	15.32	15.62

**Table 3.** The  $k_1$ ,  $k_2$ ,  $K_E$  and  $K'_E$  values for the substitution reaction.

Ligands	Temp.(°C)	$10^3 k_1$ (s <sup>-1</sup> )	$K_E$ (dm <sup>3</sup> mol <sup>-1</sup> )	$10^5 k_2$ (s <sup>-1</sup> )	$K'_E$ (dm <sup>3</sup> mol <sup>-1</sup> )
L-L <sup>1</sup> H	35	10.89(±.004)	241(±.007)	15.20(±.001)	259(±.003)
	40	12.48(±.004)	304(±.007)	18.80(±.004)	338(±.008)
	45	13.06(±.006)	360(±.010)	21.72(±.003)	343(±.005)
	50	14.28(±.003)	460(±.006)	28.33(±.002)	362(±.003)
L-L <sup>2</sup> H	35	10.15(±.004)	262(±.007)	14.30(±.003)	264(±.005)
	40	11.42(±.004)	327(±.008)	18.28(±.006)	283(±.012)
	45	12.86(±.004)	355(±.009)	21.29(±.003)	297(±.005)
	50	14.08(±.003)	467(±.006)	27.21(±.002)	336(±.004)
L-L <sup>3</sup> H	35	9.87(±.004)	268(±.007)	14.06(±.003)	255(±.005)
	40	11.10(±.003)	289(±.005)	18.09(±.005)	266(±.009)
	45	12.55(±.007)	336(±.012)	20.79(±.003)	297(±.006)
	50	13.70(±.004)	456(±.008)	26.87(±.003)	334(±.006)

**Figure 7.** Eyring plot for  $k_2$  (For L-L<sup>1</sup>H)**Figure 8.** Plot of  $\ln K_E$  Vs  $1/T$  (For L-L<sup>1</sup>H).**Table 4.** Activation parameters for  $[(H_2O)(tap)_2RuORu(tap)_2(H_2O)]^{2+}$  by various ligands in aqueous medium, pH = 7.4.

Ligand	$\Delta H_1^\ddagger$ (kJ mol <sup>-1</sup> )	$\Delta S_1^\ddagger$ (JK <sup>-1</sup> mol <sup>-1</sup> )	$\Delta H_2^\ddagger$ (kJ mol <sup>-1</sup> )	$\Delta S_2^\ddagger$ (JK <sup>-1</sup> mol <sup>-1</sup> )	Ref.
Glycyl-glycine	11.5 ± 1.6	-245 ± 5	30.2 ± 4	-220 ± 12	*
Glycyl-L-alanine	14.9 ± 0.4	-235 ± 1	31.3 ± 3.1	-217 ± 10	*
Glycyl-L-leucine	15.8 ± 0.6	-232 ± 2	31.7 ± 3.5	-216 ± 10	47

\* = This work



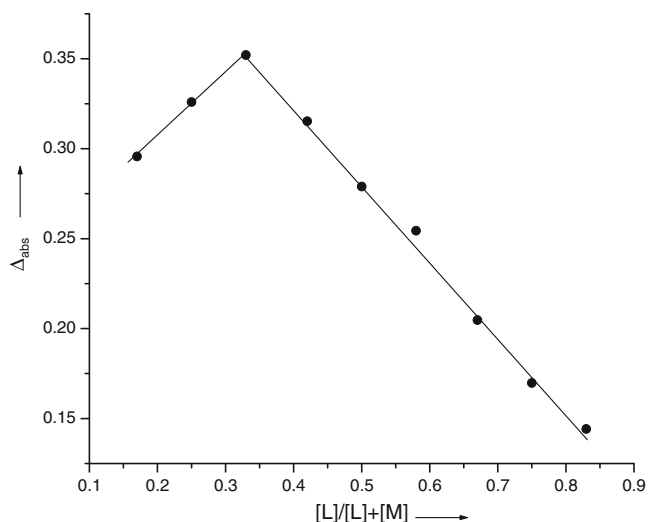


**Figure 9.** Job's plot for reaction of complex (I) with glycyl-glycine.

$k_2$  are sensitive to changes of temperature. The activation parameters for both the steps (1)  $\xrightarrow{k_1}$  (2) and (1)  $\xrightarrow{k_2}$  (2) were evaluated from the linear Eyring plots (figures 6, 7 and 8) and was compared with other systems (table 4).

The low  $\Delta H^\ddagger$  values are in support of the ligand participation in the transition state for both the steps. The energy required to break the metal-departing ligand bond is partly compensated due to the formation of metal-incoming ligand bond and a lower value of  $\Delta H^\ddagger$  is observed. The high negative  $\Delta S^\ddagger$  values suggest a more compact transition state, where both the incoming and departing ligands are attached in the transition state, and this is also in support of the assumption of a ligand

participated transition state. The  $\Delta H^\ddagger$  and  $\Delta S^\ddagger$  values are in good agreement with the previously studied systems<sup>48–52</sup> that also substantiate our study.

#### 4.4 Product analysis

The composition in the solution was determined by Job's method of continuous variation. The metal: ligand ratio was found to be 2:1 (figure 9). This is possible only when a bridged product is formed (see conclusion section).

Complex (I) and glycyl-glycine (L-L<sup>1</sup>H) were mixed in 2:1 molar ratio at pH 7.4 and a violet product was obtained. Then the product is characterized by IR and ESI-MS measurements.

The IR spectra of the violet product in the KBr disc show strong bands at  $3400\text{ cm}^{-1}$  together with medium bands at  $1618, 1600, 1400, 1109$  and  $626\text{ cm}^{-1}$ . The strong bands at  $3400\text{ cm}^{-1}$  indicate that the product is hydrated and the free carboxylic acid group is present in the product. The absorption at  $1600\text{ cm}^{-1}$  and  $1400\text{ cm}^{-1}$  due to antisymmetric stretching and symmetric stretching of  $\text{COO}^-$  group of the ligands. So we can say that  $\text{COO}^-$  group of the dipeptide is not involved in bonding with Ruthenium atoms. An intense band of the  $\nu(\text{CO})_{\text{amide}}$  at  $1665\text{ cm}^{-1}$  in the non-coordinated glycyl-glycine undergoes a bathochromic  $\sim 47\text{ cm}^{-1}$  shift in the IR spectra upon complexation. This is probably due to the involvement of the peptide nitrogen (because of the deprotonation that has taken place) in bonding with Ru(II), which lowers the bond order of the  $\nu(\text{CO})_{\text{amide}}$  group due to resonance stabilization.<sup>53</sup> The absence of stretching frequency in the region  $3000\text{--}3200\text{ cm}^{-1}$  indicates that there is no

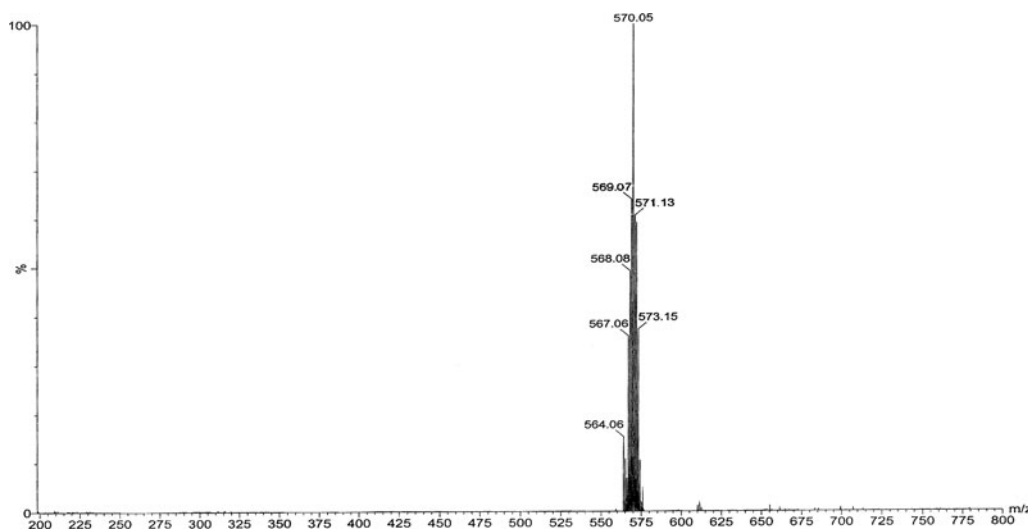


**Figure 10.** ESI-mass spectra of the product.

amide  $-N-H$  bond is present in the product. The sharp peak at  $1109\text{ cm}^{-1}$  indicates the counter anion ( $\text{ClO}_4^-$ ). The  $626\text{ cm}^{-1}$  is due to the formation of  $\text{Ru}-\text{N}$  bond in the product.<sup>54</sup>

The aqueous solution of  $[(\text{H}_2\text{O})(\text{tap})_2\text{RuORu}(\text{tap})_2(\text{H}_2\text{O})]^{2+}$  and glycyl-glycine were mixed in a 2:1

molar ratio and the mixture was thermostated at  $50^\circ\text{C}$  for 72 h and used for ESI-MS measurement. The ESI mass spectra of the resulting solution are shown in figure 10.

It is clear from this spectrum that the ion at  $m/z \sim 570$  has become the molecular ion species in the solution

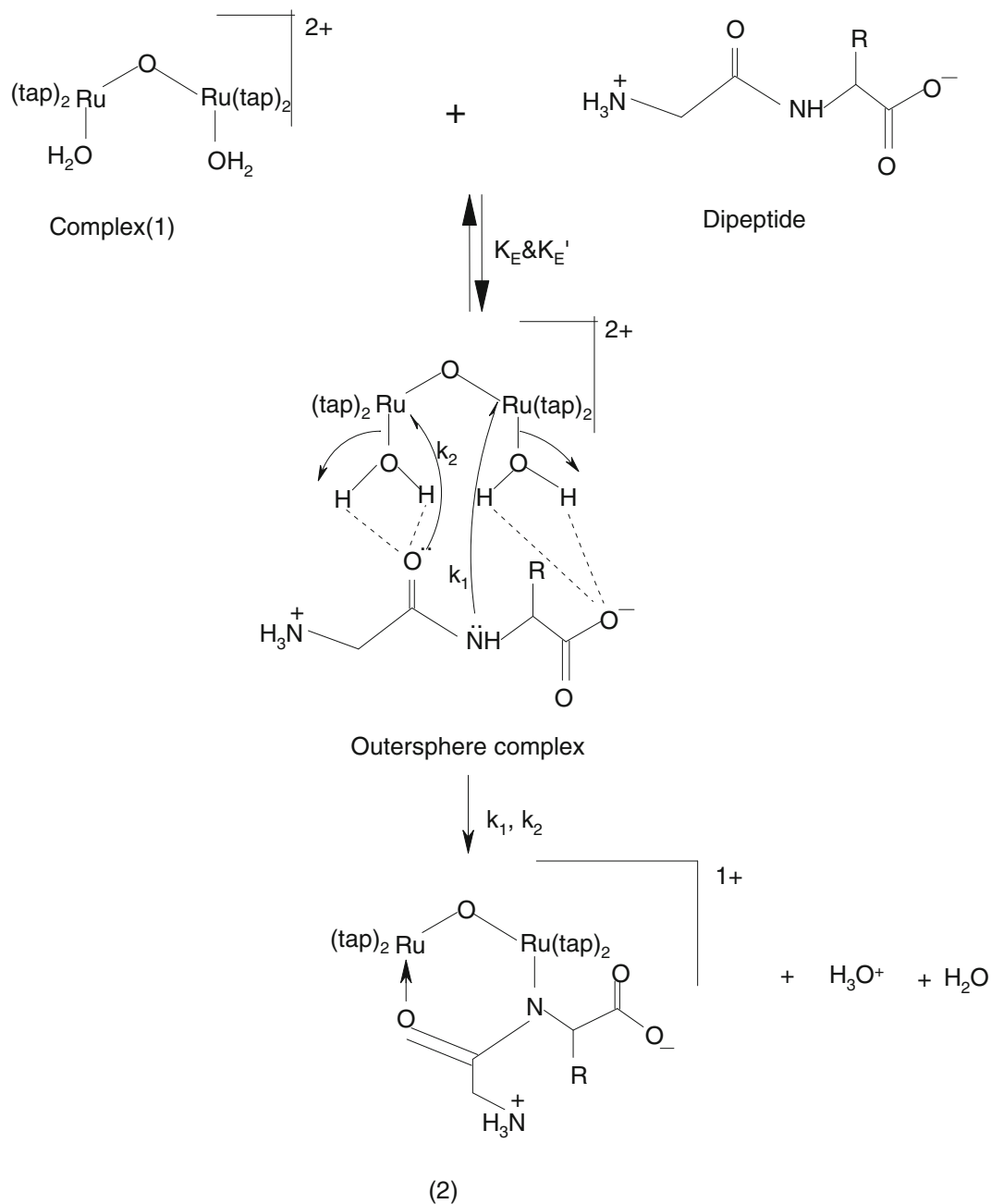


**Figure 11.** Plausible mechanism for the substitution of aqua ligands from  $[(\text{H}_2\text{O})(\text{tap})_2\text{RuORu}(\text{tap})_2(\text{H}_2\text{O})]^{2+}$  by studied dipeptides.



mixture and this is attributed to  $(\text{glycyl-glycine} - \text{H}^+ + 2\text{Ru} + 4 \text{ tap} + 1\text{O} + \text{H}^+)^{2+}$ .

#### 4.5 Physical measurements

All the spectra and kinetic measurements were recorded with a Shimadzu UV-VIS spectrophotometer (UV-1601 PC), attached to a thermoelectric cell temperature controller (model TCC-240A with an accuracy of  $\pm 0.1^\circ\text{C}$ ). IR Spectra (KBr disc,  $4000 - 300 \text{ cm}^{-1}$ ) were measured with a Perkin-Elmer FTIR model RX1 Infrared spectrophotometer. ESI-mass spectra recorded using a micro mass Q-Tof micro<sup>TM</sup> mass spectrometer in +ve ion mode. The pHs of the solutions were adjusted with  $\text{HClO}_4/\text{NaOH}$  and measured with a Sartorius pH metre (model PB11) with an accuracy of  $\pm 0.01$ . We did not add any buffer as the dipeptide in its zwitter ionic form acts as a buffer.

### 5. Conclusion

The interaction of dipeptides with the title ruthenium complex proceeds via two distinct parallel paths ( $k_1 \sim 10^{-3} \text{ s}^{-1}$  and  $k_2 \sim 10^{-5} \text{ s}^{-1}$ ). Each path proceeds via an associative interchange activation. At the outset of each path outer sphere association complex results, this is stabilized through H-bonding and is followed by an interchange from the outer sphere to the inner sphere complex. A plausible mechanism is shown in figure 11. The outer sphere association equilibrium constants, a measure of the extent of H-bonding for each path at different temperatures are evaluated (table 3).  $K_E$  and  $K'_E$  are dependent on temperature. With increase in temperature both  $K_E$  and  $K'_E$  values increase which also substantiate the proposed mechanism as with increase in temperature more and more molecules can form outer sphere association complex easily which results faster rate. From the temperature dependence of the  $K_E$  and  $K'_E$  the thermodynamic parameters are calculated:  $\Delta H_1^0 = 34.6 \pm 3.5$ ,  $30.9 \pm 4.3$  and  $25.8 \pm 7.7 \text{ kJ mol}^{-1}$ ,  $\Delta S_1^0 = 158 \pm 11$ ,  $147 \pm 14$  and  $115 \pm 24 \text{ J K}^{-1} \text{ mol}^{-1}$  and  $\Delta H_2^0 = 17.4 \pm 5.4$ ,  $12.1 \pm 2.8$  and  $11.6 \pm 2.9 \text{ kJ mol}^{-1}$ ,  $\Delta S_2^0 = 103 \pm 17$ ,  $86 \pm 9$  and  $162 \pm 9 \text{ JK}^{-1} \text{ mol}^{-1}$ , glycyl-L-alanine (L-L<sup>2</sup>H) and glycyl-L-leucine (L-L<sup>3</sup>H), respectively.  $\Delta G^0$  values, calculated for both steps at all temperatures studied, have a negative magnitude which is once again in favour of the spontaneous formation of an outersphere association complex. The six membered structure of the product is also possible by the coordination of two O atoms of carboxylate group with the two Ru(II) centres. But from the infrared study it was confirmed that the carboxylic

acid group of the dipeptides remains free and amide N and O atoms react to form the six-membered rings. Now as the N atom is softer than O atom it may be considered that the N-atom would follow the  $k_1$  path and O-atom would follow the  $k_2$  path. The N-protons on the  $-\text{NH}_3^+$  is abstracted by the  $\text{COO}^-$  group to form the final product.

From a comparison of the dipeptides used, it can be concluded that the variation in size, bulkiness and electronic effect of the entering dipeptides reflect their properties as nucleophiles. The differences in reactivity of the selected dipeptides is obvious and their reactivity follows the order Gly-L-leu < Gly-L-ala < Gly-gly i.e., with increasing steric effects reactivity decreases which is reflected in their rate constants values.

### References

1. Sadler P J 1991 *Adv. Inorg. Chem.* **36** 1
2. Clarke M J 2003 *Coord. Chem. Rev.* **236** 209
3. Guo Z and Sadler P J 1999 *Angew. Chem., Int. Ed.* **38** 1512
4. Guo Z and Sadler P J 2000 *Adv. Inorg. Chem.* **49** 183
5. Cleare M J and Hoeschele J D 1973 *Bioinorg. Chem.* **2** 187
6. Murdoch R D and Pepys J 1985 *Int. Arch. Allergy Appl. Immunol.* **77** 456
7. Clarke M J, in: A E Martell (eds.), 1980 *Inorganic chemistry in biology and medicine*, (ACS Symp. Ser. 140) American Chemical Society, Washington DC, 157 and references cited therein
8. Pruchnik P F, Bien M, Lachowicz T and Tadeusz 1996 *Met. Based Drugs* **4** 185
9. Clarke M J 1980 *Met. Ions Biol. Syst.* **11** 231
10. Yasbin R E, Matthews C R and Clarke M J 1980 *Chem. Biol. Interact.* **31** 355
11. Reedijk J 1987 *Pure Appl. Chem.* **59** 181
12. Zhao M and Clarke M J 1999 *J. Biol. Chem.* **4** 325
13. Galardon E, Maux P Lc, Bondon A and Simonncaux G 1999 *Tetrahed. Asymm.* **10** 4203
14. Frasca D R and Clarke M J 1999 *J. Am. Chem. Soc.* **121** 8523
15. Povsc V G and Olabe J A 1998 *Transition Met. Chem.* **23** 657
16. Izumi H K and Smith W L 2000 *Abstracts of papers of the Am. Chem. Soc.* **219** 727
17. Wang Z M and Ji L N 2002 *Prog. Chem.* **14** 296
18. Roncaroli F, Ruggiero M E, Franco D W, Estiu G L and Olabe J A 2002 *Inorg. Chem.* **41** 5760
19. Harthmann M, Lipponer K-G and Keppler B K 1998 *Inorg. Chim. Acta* **267** 137
20. Turel I, Pecanac M, Golobic A, Allesio E and Serli B 2002 *Eur. J. Inorg. Chem.* 1928
21. Leudtke N W, Hwang J S, Glazer E C, Gut D, Kol M and Tor Y 2002 *ChemBiochem* **3** 766
22. Shailendra Bharti N, Garza M T G, Guzvega D E, Garza J C, Saliem K, Naqv M and Zam A 2001 *Bioorg. Med. Chem. Lett.* **11** 2675

23. Alessio E, Iengo E, Serli B, Mestroni G and Sava G 2001 *J. Inorg. Biochem.* **86** 21
24. Ang W H and Dyson P J 2006 *Eur. J. Inorg. Chem.* 4003
25. Clarke M J 2003 *Coord. Chem. Rev.* **236** 209
26. Komeda S, Moulaei T, Woods K K, Chikuma M, Farrell N P, Williams L D 2006 *J. Am. Chem. Soc.* **128** 16092
27. Hannon M J 2007 *Chem. Soc. Rev.* **36** 280
28. Pitteri C and Cini R 1998 *J. Chem. Soc. Dalton Trans.* 2679
29. Sulu M, Kucukbay H, Durmaz R and Gunal S 2000 *Microbiologica* **23** 73
30. Bratsos I, Jedner S, Gianferrara T and Alessio E 2007 *Metals Med.* **61** 692
31. Ghosh B K and Chakravorty A 1989 *Coord. Chem. Rev.* **95** 239
32. Goswami S, Chakraborty A R and Chakravorty A 1981 *Inorg. Chem.* **20** 2246
33. Goswami S, Chakraborty A R and Chakravorty A 1983 *Inorg. Chem.* **22** 603
34. Weyh J A and Hamm R E 1969 *Inorg. Chem.* **8** 2298
35. Kim M K and Martell A E 1984 *Biochemistry* **3** 1169
36. Sigel H, Griesser R and Prijs B 1972 *Z. Naturforsch. (B)*, **27** 353
37. Martell A E and Smith R M 1974 *Critical stability constants*, vol. 1, New York, NY, USA: Plenum Press, 297
38. Martell A E and Smith R M 1974 *Critical stability constants*, vol. 1, New York, NY, USA: Plenum Press, 299
39. Mahanti B and De G S 1992 *Transition Met. Chem.* **17** 521
40. Raven S J and Meyer T J 1998 *Inorg. Chem.* **27** 4478
41. Kutner W, Gilbert J A, Tomaszewski A, Meyer T J and Murray R W 1986 *J. Electroanal. Chem.* **205** 185
42. Gersten S W, Samuels G J and Meyer T J 1982 *J. Am. Chem. Soc.* **104** 4029
43. Ghosh P and Chakravorty A 1984 *Inorg. Chem.* **23** 2242
44. Cotton F A, Wilkinson G, Murrilo C A and Bochman M 1999 *Adv. Inorg. Chem.*, New York, NY, USA: John Wiley & Sons, 6th edition
45. Gilbert J A, Eggleston D S, Murphy W R Jr et al 1985 *J. Am. Chem. Soc.* **107** 3855
46. Gilbert J A, Geselowitz D and Meyer T J 1986 *J. Am. Chem. Soc.* **108** 1493
47. Mandal A, Mallick S, Karmakar P, Bera B K, Mondal S and Ghosh A K 2012 *Prog React. Kinet. Mech.* **37** 1.
48. Chattopadhyay H, Ghosh A K and Ghosh B K 2004 *Transition Met. Chem.* **29** 24
49. Chattopadhyay H, Ghosh A K and Ghosh B K 2004 *Inorg. React. Mech.* **5** 87
50. Chattopadhyay H and Ghosh A K 2005 *Indian J. Chem.* **44A** 483
51. Chattopadhyay H and Ghosh A K 2006 *Inorg. React. Mech.* **6** 9
52. Ghosh A K 2006 *Transition Met. Chem.* **31** 912
53. Nath M, Pokharia S, Eng G, Song X and Kumar A 2004 *Synth. React. Inorg. Met. Chem.* **34** 1689
54. Mercer E E, McAllister W A and Durig J R 1966 *Inorg. Chem.* **5** 1881